Nitrogen−Nitrogen Bond Cleavage of Hydrazine Derivatives by a Trinuclear Pentahydride Complex of Ruthenium, $(Cp'Ru)_3(\mu\text{-}H)_3(\mu_3\text{-}H)_2$ ($Cp' = \eta^5\text{-}C_5Me_5$)

Yumiko Nakajima and Hiroharu Suzuki*

Department of Applied Chemistry, Graduate School of Science and Engineering, Tokyo Institute of Technology, and CREST, Japan Science and Technology Corporation (JST), O-okayama, Meguro-ku, Tokyo 152-8552, Japan

Received September 11, 2002

The reaction of $(Cp'Ru)_3(\mu\text{-}H)_3(\mu_3\text{-}H)_2$ (**1**) with a monosubstituted hydrazine such as methylhydrazine and phenylhydrazine results in the exclusive formation of the nonsymmetrically capped bis(μ_3-imido) complex $(Cp'Ru)_3(\mu_3\text{-}NR)(\mu_3\text{-}NH)(\mu\text{-}H)$ (**2**, R = Me; **3**, R = Ph) as a result of cleavage of the nitrogen−nitrogen bond. In contrast to the reaction with monosubstituted hydrazine, the reaction of **1** with 1,2-diphenylhydrazine predominantly yields the monocapped imido complex $(Cp'Ru)_3(\mu_3\text{-}NPh)(\mu\text{-}H)_3$ (**4**), due to the steric hindrance between the Cp′ groups surrounding the reaction site of **1** and the incoming bulky 1,2-diphenylhydrazine. Kinetic studies were carried out to elucidate the reaction mechanism and proved that the methylhydrazine molecule was captured by the Ru_3 site from the more nucleophilic −NHMe terminus rather than the less bulky $-NH_2$ terminus. Molecular structures of **2**−**4** and $(Cp'Ru)_3(\mu_3\text{-}NH)_2(\mu\text{-}H)$ (**6**) have been determined by means of X-ray diffraction studies.

Introduction

The metal hydrazido species is an intermediate of the reduction of dinitrogen to ammonia catalyzed by nitrogenase. As a model system of nitrogen fixation by nitrogenase, reaction of transition-metal complexes, particularly the complexes of early or middle transition metals, with dinitrogen has been thus far extensively studied.[1] Protonation of metal-bound dinitrogen leads to the formation of complexes containing a N_2 fragment such as the diazenido (NNH) or hydrazido(2−) ligand (NNH_2).[2] Successive protonation and subsequent electron transfer from the reducing agent achieve reduction of these ligands to produce ammonia.[3] These diazenido and hydrazido(2−) ligands are closely related to hydrazine coordinated to the transition-metal complex, and study of the reaction chemistry of the hydrazine complexes is, therefore, helpful to elucidate details of the transition-metal-assisted nitrogen reduction. So far, extensive research has been done on the reaction of a transition-metal complex with hydrazine or substituted hydrazine to elucidate how the nitrogen−nitrogen bond is cleaved by a transition-metal complex.[4]

Schrock et al. have prepared a number of cationic hydrazine complexes such as $[Cp'WMe_3(\eta^2\text{-}NH_2NH_2)]^+$,[5] $[Cp'MoMe_3(\eta^2\text{-}NH_2NH_2)]^+$,[6] $[Cp'ReMe_3(\eta^2\text{-}NH_2NH_2)]^+$,[7] and $[Cp'WMe_4(\eta^2\text{-}NH_2NH_2)]^+$[8] by the reaction of the corresponding unsaturated cationic complex $Cp'MMe_n(OTf)$ (n = 3, 4) with hydrazine and showed that the nitrogen−nitrogen bond in coordinated hydrazine was efficiently cleaved by the treatment with zinc amalgam

* To whom correspondence should be addressed.

(1) For example: (a) Chatt, J.; Dilworth, J. R.; Richards, R. L. *Chem. Rev.* **1978**, *78*, 590. (b) Hidai, M.; Mizobe, Y. *Chem. Rev.* **1995**, *95*, 1115. (c) LaPlaza, C. E.; Cummins, C. C. *Science* **1995**, *268*, 861. (d) Fryzuk, M. D.; Johnson, S. A.; Rettig, S. T. *J. Am. Chem. Soc.* **1998**, *120*, 11024. (e) Nishibayashi, Y.; Takemoto, S.; Iwai, S.; Hidai, M. *Inorg. Chem.* **2000**, *39*, 5946. (f) Greco, G. E.; Schrock, R. R. *Inorg. Chem.* **2001**, *40*, 3861. (g) Fryzuk, M. D.; Johnson, S. A. *Coord. Chem. Rev.* **2000**, *200*−*202*, 379. (h) Clemtsmith, G. K. B.; Bates, V. M. E.; Hitchcock, P. B.; Cloke, F. G. N. *J. Am. Chem. Soc.* **1999**, *121*, 10444. (i) Zanotti-Gerosa, A.; Solari, E.; Giannini, L.; Floriani, C.; Chiesi-Villa, A.; Rizzoli, C. *J. Am. Chem. Soc.* **1998**, *120*, 437. (j) Ferguson, R.; Solari, E.; Floriani, C.; Osella, D.; Ravera, M.; Re, N.; Chiesi-Villa, A.; Rizzoli, C. *J. Am. Chem. Soc.* **1997**, *119*, 10104.

(2) For example: (a) Chatt, J.; Heath, G. A.; Richards, R. L. *J. Chem. Soc., Dalton Trans.* **1974**, 2074. (b) George, T. A.; Kaul, B. B. *Inorg. Chem.* **1991**, *30*, 882. (c) Ishii, Y.; Miyagi, H.; Jitukuni, S.; Seino, H.; Harkness, B. S.; Hidai, M. *J. Am. Chem. Soc.* **1992**, *114*, 9890. (d) Yamabe, T.; Hori, K.; Fukui, K. *Inorg. Chem.* **1982**, *21*, 2046.

(3) For example: (a) George, T. A.; Rose, D. J.; Chang, Y.; Chen, Q.; Zubieta, J. *Inorg, Chem.* **1995**, *34*, 1295. (b) Shilov, A. E. *Pure Appl. Chem.* **1992**, *64*, 1409. (c) Hall, D. A.; Leigh, G. J. *J. Chem. Soc., Dalton Trans.* **1996**, 3539. (d) Ishino, H.; Nagano, T.; Kuwata, S.; Yokobayashi, Y.; Ishii, Y.; Hidai, M.; Mizobe, Y. *Organometallics* **2001**, *20*, 188. (e) Feruston, R.; Solari, E.; Floriani, C.; Osella, D.; Ravera, M.; Re, N.; Chiesi-Villa, A.; Rizzoli, C. *J. Am. Chem. Soc.* **1997**, *119*, 10104. (f) Leigh, G. J.; Prieto-Alcón, R.; Sanders, J. R. *J. Chem. Soc., Chem. Commun.* **1991**, 921. (g) Baumanm, J. A.; George, T. A. *J. Am. Chem. Soc.* **1980**, *102*, 6153. (h) Yamamoto, A.; Miura, Y.; Ito, T.; Chen, H.-L.; Iri, K.; Ozawa, F.; Miki, K.; Sei, T.; Tanaka, N.; Kasai, N. *Organometallics* **1983**, *2*, 1429. (i) Anderson, S. N.; Hughes, D. L.; Richards, R. R. *J. Chem. Soc., Dalton Trans.* **1986**, 1591.

(4) For example: (a) Heaton, B. T.; Jacob, C.; Page, P. *Coord. Chem. Rev.* **1996**, *154*, 193. (b) Jahncke, M.; Neels, A.; Stoeckli-Evans, H.; Vale, M. G.; Süss-Fink, G. *J. Organomet. Chem.* **1998**, *565*, 97. (c) Malinak, S. M.; Demadis, K. D.; Coucouvanis, D. *J. Am. Chem. Soc.* **1995**, *117*, 3126. (d) Kuwata, S.; Mizobe, Y.; Hidai, M. *Inorg. Chem.* **1994**, 3619.

(5) Schrock, R. R.; Glassman, T. E.; Vale, M. G.; Kol, M. *J. Am. Chem. Soc.* **1993**, *115*, 1760.

(6) (a) Schrock, R. R.; Glassman, T. E.; Vale, M. G. *J. Am. Chem. Soc.* **1991**, *113*, 725. (b) Vale, M. G.; Schrock, R. R. *Inorg. Chem.* **1993**, *12*, 1140.

(7) (a) Vale, M. G.; Schrock, R. R. *Organometallics* **1991**, *10*, 1661. (b) Vale, M. G.; Schrock, R. R. *Organometallics* **1993**, *12*, 1140.

(8) Schrock, R. R.; Liu, A. H.; O'Regon, M. B.; Finch, W. C.; Payack, J. F. *Inorg. Chem.* **1988**, *27*, 3574.

10.1021/om020755+ CCC: $25.00
Publication on Web 01/28/2003

in the presence of 2,6-lutidine hydrochloride.[5] Cleavage of the nitrogen−nitrogen bond of hydrazine was also achieved using a dinuclear thiolato-bridged complex of molybdenum, $Cp_2Mo_2(\mu\text{-}SMe)_3$ (Cp = η^5-C_5H_5), discovered by Pétillon, Muir, and co-workers.[9] They also investigated the transformation of hydrazine derivatives such as phenylhydrazine and azobenzene to gain a deep insight into the mechanism of the nitrogen−nitrogen bond cleavage of hydrazine.[10] Süss-Fink et al. studied the reaction of the cationic dinuclear ruthenium hydride complex $[(\eta^6\text{-}C_6Me_6)_2Ru_2(\mu\text{-}H)_3]^+$ with hydrazine and reported the formation of the dinuclear μ-imido complex $[(\eta^6\text{-}C_6Me_6)_2Ru_2(\mu\text{-}\eta^1\text{:}\eta^1\text{-}NH_2NH_2)(\mu\text{-}NH_2)(\mu\text{-}H)]^{2+}$ together with ammonia as a result of the nitrogen−nitrogen bond cleavage of the intermediary $[(\eta^6\text{-}C_6Me_6)_2Ru_2(\mu\text{-}\eta^1\text{:}\eta^1\text{-}NH_2NH_2)(\mu\text{-}NHNH_2)(\mu\text{-}H)]^{2+}$.[4b]

Thus, the nitrogen−nitrogen bond cleavage of hydrazine and its derivatives by a transition-metal complex is an interesting and important step in relation to the nitrogen reduction to ammonia.

We have so far studied the reaction chemistry of the di- and trinuclear ruthenium polyhydride clusters $(Cp'Ru)_2(\mu\text{-}H)_4$ and $(Cp'Ru)_3(\mu\text{-}H)_3(\mu_3\text{-}H)_2$ and shown that the carbon−hydrogen bond of alkanes and even the carbon−carbon double bond of 1,1-disubstituted alkenes are readily cleaved due to cooperative action of the adjacent metal atoms.[11] Since a metal polyhydride cluster not only has many hydrogen atoms in the core of the cluster but also has an intrinsic property of transferring multiple electrons between the cluster and the coordinated substrate, the polyhydride cluster likely promotes the nitrogen reduction to ammonia in the absence of both a proton source and a reducing agent.

We have studied the reaction of $(Cp'Ru)_3(\mu\text{-}H)_3(\mu_3\text{-}H)_2$ (**1**) with hydrazine derivatives, such as methylhydrazine, phenylhydrazine, and 1,2-diphenylhydrazine, in detail to elucidate how the nitrogen−nitrogen bond is cleaved in the trimetallic reaction site. In this paper, we report that cleavage of the nitrogen−nitrogen bond of the above hydrazine derivatives is achieved using triruthenium pentahydride **1** and discuss the mechanistic details of the reaction.

Results and Discussion

Reaction of $(Cp'Ru)_3(\mu\text{-}H)_3(\mu_3\text{-}H)_2$ with Hydrazine Derivatives. The triruthenium pentahydride complex $(Cp'Ru)_3(\mu\text{-}H)_3(\mu_3\text{-}H)_2$ (**1**) is reactive toward a monosubstituted hydrazine such as methylhydrazine and phenylhydrazine, but the reaction proceeds very slowly at ambient temperature. Elevation of the reaction temperature is needed to complete the reaction.

Treatment of **1** with 34 equiv of methylhydrazine, $MeNHNH_2$, in tetrahydrofuran at 100 °C for 96 h resulted in the formation of the trinuclear bicapped imido complex $(Cp'Ru)_3(\mu_3\text{-}NMe)(\mu_3\text{-}NH)(\mu\text{-}H)$ (**2**) as a major product. Purification by means of column chromatography on alumina gave **2** as a red solid in 75% isolated yield (eq 1).

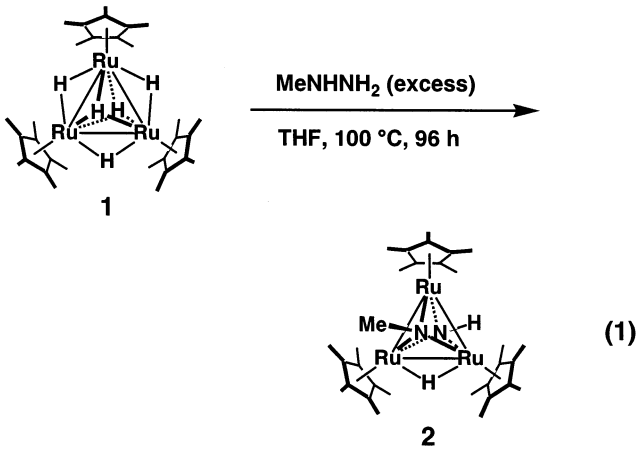

(1)

As mentioned below, each face of the Ru_3 core of **2** is capped with a different kind of triply bridging imido ligand, μ_3-NMe and μ_3-NH, respectively. It is noteworthy that the homobicapped imido complexes $(Cp'Ru)_3(\mu_3\text{-}NH)_2(\mu\text{-}H)$ (**6**)[12] and $(Cp'Ru)_3(\mu_3\text{-}NMe)_2(\mu\text{-}H)$ (**7**) were not formed at all in this reaction.

The mixed-bicapped imido complex **2** was unambiguously identified on the basis of the ^1H and ^{13}C NMR data as well as elemental analysis. The ^1H NMR spectrum exhibits a broad signal ($w_{1/2}$ = 59.3 Hz) with an integral intensity of 1H assignable to the proton attached to the triply bridging nitrogen atom at significantly low field, δ 13.06. This chemical shift is characteristic of a μ_3-imido ligand coordinated to the $(Cp'Ru)_3$ core, such as $(Cp'Ru)_3(\mu_3\text{-}NH)_2(\mu\text{-}H)$ (**6**; δ 12.98) and $(Cp'Ru)_3(\mu_3\text{-}NH)(\mu\text{-}H)_3$ (**8**; δ 13.69).[13] The signals of the μ_3-NMe and hydride ligands appeared as singlets at δ 4.24 and −19.15, respectively, in an intensity ratio of 3:1. The signals of the Cp′ groups were observed at δ 1.79 (30H) and 1.85 (15H), and this result strongly indicated that complex **2** has a symmetry plane vertical to the Ru_3 core. The C_s-symmetrical structure of **2** was established by an X-ray diffraction study (vide infra).

Even in the low distribution, formation of three intermediates was observed when the reaction of **1** with methylhydrazine in tetrahydrofuran-d_8 was monitored by means of ^1H NMR spectroscopy. One of them converged into **2**, and the others were converted to minor side products.

The reaction of **1** with phenylhydrazine was also carried out under similar conditions. The reaction of **1** with an excess amount (26 equiv) of phenylhydrazine in tetrahydrofuran at 100 °C for 6 h led to the quantitative formation of the mixed-bicapped imido complex $(Cp'Ru)_3(\mu_3\text{-}NPh)(\mu_3\text{-}NH)(\mu\text{-}H)$ (**3**), which was isolated by using column chromatography on alumina and identified on the basis of the ^1H and ^{13}C NMR spectral data (eq 2). As observed in the reaction of **1** with methylhydrazine, neither of the homobicapped imido complexes $(Cp'Ru)_3(\mu_3\text{-}NH)_2(\mu\text{-}H)$ (**6**) and $(Cp'Ru)_3(\mu_3\text{-}NPh)_2(\mu\text{-}H)$ (**5**) was formed in this reaction.

(9) Schollhammer, P.; Pétillon, F. Y.; Poder-Guillou, S.; Saillard, J. Y.; Talarmin, J.; Muir, K. W. *Chem. Commun.* **1996**, 2633.

(10) (a) Schollhammer, P.; Guénin, E.; Pétillon, F. Y.; Talarmin, J.; Muir, K. W.; Yufit, D. S. *Organometallics* **1998**, *17*, 1922. (b) Pétillon, F. Y.; Scholhammer, P.; Talarmin, J.; Muir, K. W. *Inorg, Chem.* **1999**, *38*, 1954.

(11) (a) Suzuki, H. *Eur. J. Inorg. Chem.* **2002**, 1009. (b) Ohki, Y.; Suzuki, H. *Angew. Chem.* **2000**, *39*, 3463. (c) Inagaki, A.; Takemori, T.; Tanaka, M.; Suzuki, H. *Angew. Chem.* **2000**, *39*, 404. (d) Takemori, T.; Inagaki, A.; Suzuki, H. *J. Am. Chem. Soc.* **2001**, *123*, 1762.

(12) As mentioned below, complex **6** was prepared from the reaction of **8** with methylhydrazine in tetrahydrofuran.

(13) Matsubara, K.; Suzuki, H. Manuscript in preparation.

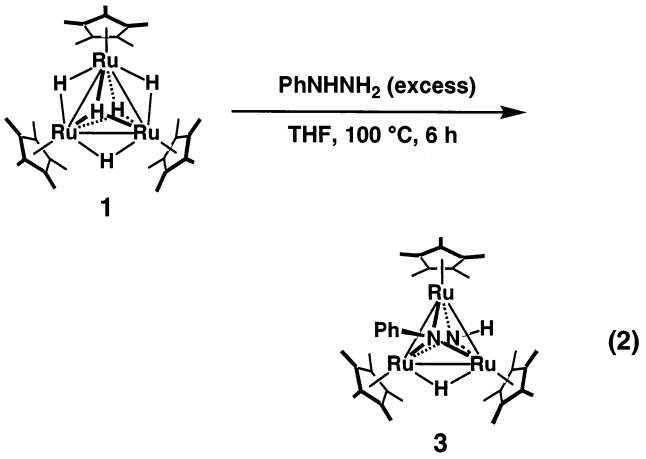

(2)

In the ^{1}H NMR spectrum, the signal for the μ_3-NH ligand appeared at δ 13.67 as a broad peak with $w_{1/2}$ = 34.1 Hz, and a phenyl group bound to the triply bridging nitrogen atom was observed in the region of δ 6.7−7.0. The signals of the phenyl protons shift significantly to upper field as compared to those of the ordinary aromatic protons. This is probably due to the shielding effect of the aromatic ring current of the three Cp′ rings, since the phenyl group is located above the center of the Ru_3 triangle. A sharp singlet peak assignable to the hydride ligand was observed at δ −18.93.

One most important feature observed in the reaction of **1** with monosubstituted hydrazine is the selective formation of a mixed-bicapped imido complex that has two different kinds of μ_3-imido ligands on each face of the Ru_3 plane. Formation of both monocapped and homobicapped imido complexes was not observed at all. This strongly implies that both of the two μ_3-imido ligands, μ_3-NH and μ_3-NR, introduced into the Ru_3 core are derived from one molecule of the substituted hydrazine.

Monitoring the reaction by spectroscopic techniques is very helpful for elucidating the reaction mechanism. When the reaction of **1** with a large excess amount (34 equiv) of phenylhydrazine was carried out in tetrahydrofuran-d_8 at 100 °C and monitored by ^{1}H NMR spectroscopy, a set of signals of the intermediate **X** was observed together with those of the mixed-bicapped imido complex **3**. The time−distribution curves are shown in Figure 1.

With a decrease in the intensity of **1**, the integral intensity of the intermediate **X** increased and the distribution of the intermediate **X** reached 47% after 55 min. With the reaction time, a progressive increase in the intensity of the signal of **3** and a significant decrease in those of **I-4** were observed.

As described below, the rate of the reaction of **1** with excess phenylhydrazine is pseudo first order in the complex **1**. From the time−distribution curve shown in Figure 1, the k_2/k_1 ratio was estimated as 0.55 and the reaction step from **X** to the final product **3** was concluded to be the rate-determining step.

Although **X** could not be isolated, its structure was reasonably presumed on the basis of the ^{1}H and ^{13}C NMR spectra. Notable features observed in both the ^{1}H and ^{13}C NMR spectra are a set of signals of the Cp′ groups with an intensity ratio of 1:2. In the ^{1}H NMR spectrum, two sharp singlet peaks of the Cp′ groups

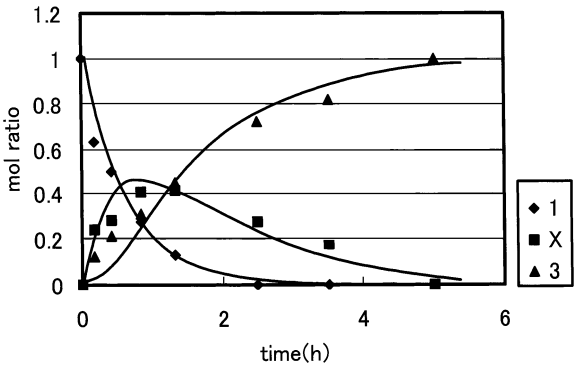

Figure 1. Time−distribution curve of the reaction of **1** with phenylhydrazine.

Chart 1. Structures for X

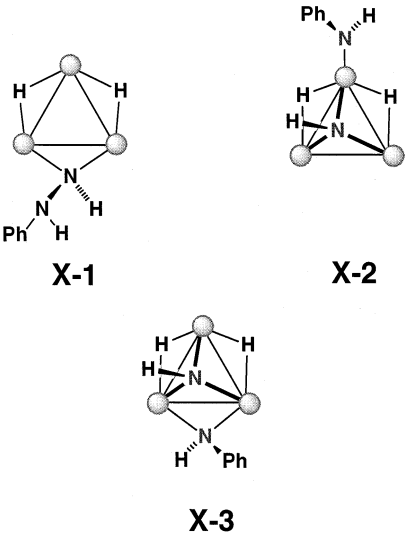

appeared at δ 1.49 (15H) and 1.96 (30H). The signals of the two hydride ligands were observed to be equivalent at δ −19.30. The signals observed at δ 7.70 (2H), 7.16 (2H), and 7.00 (1H) were assigned to the ortho, meta, and para protons of the N-bound phenyl group, respectively, on the basis of the ^{1}H−^{1}H COSY and the HMQC spectra. The proton directly attached to the nitrogen atom could not be observed, due to broadening of the peak. The ^{13}C NMR spectrum was consistent with the structure of **X** with a mirror plane vertical to the Ru_3 plane, which was suggested on the basis of the ^{1}H NMR data.

Three of the possible structures, **X-1**, **X-2**, and **X-3**, for the intermediate **X** are shown in Chart 1. **X-1** is a μ-hydrazido complex, and **X-2** is a μ_3-imido-phenylamido complex formed as a result of N−N bond cleavage of the hydrazido ligand in complex **X-1**. **X-3** has both μ_3-NH and μ-NPhH groups. Among these three structures, only **X-3** satisfies the requirement that the intermediate has the symmetry plane vertical to the Ru_3 core. We, therefore, tentatively assigned **X-3** as the structure of the intermediate. The chemical shift of δ −19.30 for the hydride ligands of **X-3** is comparable to those for hydrides in bis(μ_3-imido) complexes such as (Cp′Ru)$_3$(μ_3-NMe)(μ_3-NH)(μ-H) (**2**; δ −19.15) and (Cp′Ru)$_3$(μ_3-NH)$_2$(μ-H) (**6**; δ −19.27).

The triruthenium pentahydride **1** also reacts with 1,2-disubstituted hydrazine under similar conditions. Monitoring the reaction of **1** with an excess amount (7 equiv)

Table 1. Crystallographic Data and Measurement Conditions

	2	3	4	6
empirical formula	$C_{31}H_{50}N_2Ru_3$	$C_{36}H_{52}N_2Ru_3$	$C_{36}H_{53}NRu_3$	$C_{30}H_{48}N_2Ru_3$
fw	753.94	816.01	803.00	739.91
cryst descripn	prism	prism	prism	prism
cryst color	red	red	green	red
cryst size, mm	0.40 × 0.05 × 0.05	0.20 × 0.15 × 0.05	0.20 × 0.10 × 0.10	0.20 × 0.20 × 0.40
crystallizing soln (temp, °C)	THF (−30)	THF (−30)	toluene/pentane (−30)	THF (−30)
cryst syst	trigonal	monoclinic	monoclinic	triclinic
space group (No.)	$R\bar{3}$ (148)	$C2/m$ (12)	$C2/m$ (12)	$P\bar{1}$ (2)
lattice params				
a, Å	18.565(2)	17.5985(15)	17.489(6)	11.0087(11)
b, Å	18.565(2)	18.3862(15)	18.61(1)	11.0037(19)
c, Å	15.904(4)	11.1112(5)	11.046(5)	15.699(3)
α, deg	90.0000	90.0000	90.0000	74.785(4)
β, deg	90.0000	103.5890(16)	106.163(3)	72.418(6)
γ, deg	120.000	90.0000	90.0000	60.2500(19)
V, Å^3	4747.1(13)	3494.6(4)	3453(3)	1594.0(4)
Z	6	4	4	2
D_{calcd}, g/cm^3	1.582	1.549	1.545	1.571
measmt temp, °C	−20	−50	−50	−50
μ(Mo Kα), mm^{-1}	1.434	1.305	1.319	1.449
diffractometer	Rigaku AFC7R	R-AXIS RAPID	Rigaku AFC7R	R-AXIS RAPID
radiation (λ, Å)	Mo Kα (0.710 69)	Mo Kα (0.710 69)	Mo Kα (0.710 69)	Mo Kα (0.710 69)
monochromator	graphite	graphite	graphite	graphite
$2\theta_{max}$, deg	55	55	55	55
no. of rflns collected	2598	4048	4183	6433
no. of indep rflns	2408	4048	4057	6433
no. of rflns obsd (>2σ))	1760	3170	3538	4962
abs collecn type	ψ scan	abscor	ψ scan	abscor
abs transmissn: max, min	0.943, 1.000	0.778, 1.16	0.673, 1.000	0.661, 1.345
R1 ($I > 2\sigma(I)$)	0.0287	0.0520	0.0378	0.0777
wR2 ($I > 2\sigma(I)$)	0.0721	0.1214	0.1085	0.1656
R1 (all data)	0.0581	0.0708	0.0454	0.1055
wR2 (all data)	0.0810	0.1309	0.1153	0.1818
no. of restraints	0	0	0	0
no. of params	117	171	207	332
GOF	1.001	1.085	1.021	1.103

of 1,2-diphenylhydrazine in tetrahydrofuran-d_8 by ^{1}H NMR spectroscopy showed that **1** disappeared after standing for 30 h at 100 °C to lead to the formation of the monocapped phenylimido complex $(Cp'Ru)_3(\mu_3\text{-NPh})(\mu\text{-H})_3$ (**4**) and the homobicapped imido complex $(Cp'Ru)_3(\mu_3\text{-NPh})_2(\mu\text{-H})$ (**5**) in 91 and 9% yields, respectively, together with the formation of aniline (eq 3). No reaction

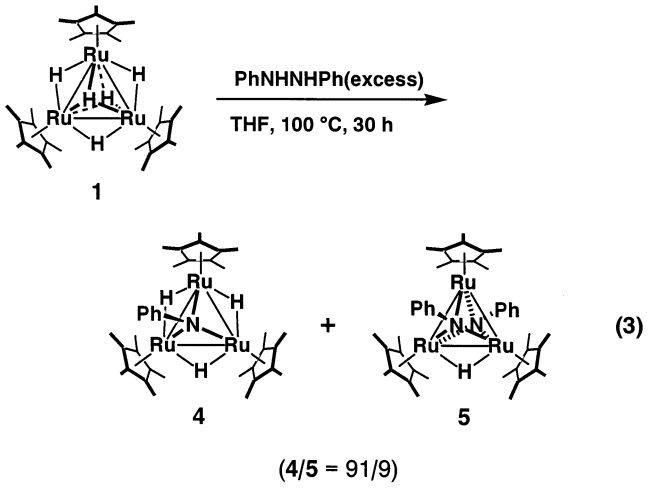

(3)

intermediate was detected in this reaction. Both products were identified on the basis of the ^{1}H and ^{13}C NMR spectra, as mentioned below.

In contrast to the reaction with a monosubstituted hydrazine such as $MeNHNH_2$ or $PhNHNH_2$, the reaction of **1** with 1,2-diphenylhydrazine predominantly yields a monocapped imido complex. This is certainly due to the steric hindrance between the Cp′ groups surrounding the reaction site of **1** and the incoming bulky substrate. Only in the presence of a large excess of 1,2-diphenylhydrazine is the homobicapped imido complex **5** formed as a minor product. A controlled experiment using **1** and 0.5 molar equiv of 1,2-diphenylhydrazine and subsequent chromatographic separation of the reaction mixture enabled us to isolate **4** as a green solid.

The ^{1}H and ^{13}C NMR spectral data of **4** are consistent with a structure with a 3-fold axis perpendicular to the Ru_3 plane. The signals of the three Cp′ groups are observed to be equivalent at δ 1.72, and those of the N-bound phenyl group appeared in the range from δ 6.5 to 7.0. The significant upfield shift of the phenyl signals is reasonably explained as due to the shielding effect by the three Cp′ rings. In contrast to the monocapped complex **4**, complex **5** has a mirror plane in its structure. The signals of the Cp′ groups are, therefore, observed at δ 1.39 and 1.72 in an intensity ratio of 1:2.

Structure Determination of the μ_3-Imido Complexes. In the reaction of **1** with mono- and 1,2-disubstituted hydrazines, novel mono-μ_3-imido and bis-(μ_3-imido) complexes are formed as a result of nitrogen−nitrogen bond cleavage. The structures of these novel μ_3-imido complexes were determined by means of X-ray diffraction studies by using single crystals obtained from cold tetrahydrofuran. The crystal data for **2**−**4** are given in Table 1. The hydrogen atoms directly bound to the ruthenium atom were not located in the differential

Table 2. Selected Interatomic Distances (Å) and Angles (deg) of 2[a]

	Distances		
Ru1−Ru1	2.7311(5)	N1−C11B	1.395(15)
Ru1−N1	1.997(3)	N2−C11A	1.421(17)
Ru1−N2	1.999(3)		
	Angles		
N1−Ru1−N2	75.81(17)	C11A−N1−Ru1	127.94(12)
N1−Ru1−Ru1	46.92(9)	Ru1−N1−Ru1	86.16(17)
N2−Ru1−Ru1	46.87(8)	Ru1−N2−Ru1	86.26(17)
C11B−N2−Ru1	127.87(12)	G1−Ru1−CEN1	179.5

[a] G1 and CEN1 are the center of gravity of the Ru_3 triangle and the centroid of Cp′, respectively.

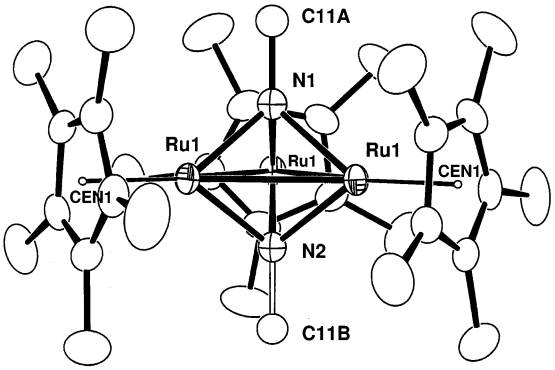

Figure 2. Molecular structure of **2**. Thermal ellipsoids are drawn at the 30% probability level.

Fourier maps in all cases. Figures 2−4 display the ORTEP diagrams of **2**−**4**, respectively. Their bond distances and angles are listed in Tables 2−4, respectively.

The structure shown in Figure 2 is fully consistent with the above-mentioned spectral data, although the two triply bridging ligands are disordered with respect to the Ru_3 plane (52.9:47.1). The hydrogen atom bound directly to the metal atoms through a two-electron−three-center (2e−3c) interaction is also disordered among the three coordination sites (33.3:33.3:33.3). Complex **2** contains μ_3-NMe and μ_3-NH ligands on each face of the Ru_3 plane, as anticipated on the basis of the ^{1}H NMR spectral data. The Ru−Ru distance of 2.7312(5) Å is significantly shorter than those of Ru−Ru single bonds (2.7497(7) Å for **1** and 2.7063(10) Å for $[(Cp'Ru)_3(\mu\text{-}H)_6](SO_4)_{1/2}$),[14] although the EAN rule applied to **2** requires a single bond between the two ruthenium atoms. This is probably due to the presence of two triply bridging imido ligands and a bridging hydride ligand. These bridging ligands would fasten three ruthenium atoms tightly and, as a result, the Ru−Ru distances probably diminish. The nitrogen atom of the μ_3-imido group is separated from the ruthenium by 1.999(3) Å. This distance is slightly longer than the sum of the covalent radii of the ruthenium (1.94 Å)[15] and nitrogen and is between the lengths of a Ru−N coordination bond (2.1−2.2 Å)[16] and a Ru−N σ bond (for example, 1.966 Å for $[(NH_3)_4(\mu\text{-}NHCOCH_2NH_2)Ru]^{2+}(PF_6)^{2-}$).[17] The Ru−N distance of **2** is consistent with a formal assignment of the triply bridged imide moiety as μ_3-NR.[18]

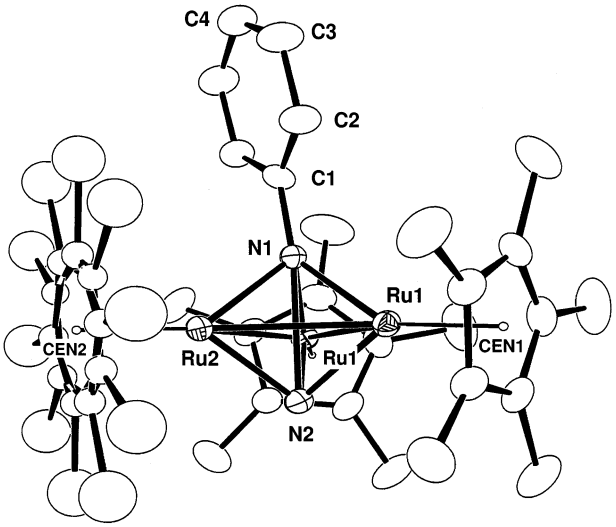

Figure 3. Molecular structure of **3**. Thermal ellipsoids are drawn at the 30% probability level.

Table 3. Selected Interatomic Distances (Å) and Angles (deg) of 3[a]

	Distances		
Ru1−Ru2	2.7387(6)	Ru1−N2	1.992(5)
Ru1−Ru1	2.7301(19)	Ru2−N2	1.988(6)
Ru1−N1	2.038(4)	N1−C1	1.411(10)
Ru2−N1	2.023(6)		
	Angles		
Ru1−N1−Ru2	84.8(2)	C1−N1−Ru1	132.6(2)
Ru1−N1−Ru1	84.1(2)	C1−N1−Ru2	121.4(5)
Ru2−N2−Ru1	87.0(2)	G1−Ru1−CEN1	174.35
Ru1−N2−Ru1	86.5(2)	G1−Ru2−CEN2	177.80

[a] G1 is the center of the gravity of the Ru_3 triangle, and CEN1 and CEN2 are the centroids of Cp.

The molecular structure of **3**, illustrated in Figure 3, clearly shows the formation of a mixed-bicapped imido complex that has μ_3-NPh and μ_3-NH groups on each face of the Ru_3 core.

The molecule has a crystallographic symmetry plane with C4, C1, N1, Ru1, and N2. The Ru_3 core makes a nearly equilateral triangle with an edge of 2.736 Å (av): this value is also slightly shorter than that of the Ru−Ru single bond and is comparable to that obtained for **2**. A notable feature of the structure of **3** is the tilt of the phenyl ring on N1. The C1−N1−Ru1 and C1−N1−Ru2 angles are 132.6(2) and 121.4(5)°, respectively, and the phenyl group tilts toward Ru2. This is probably due to steric repulsion between the hydrogen at the ortho position of the phenyl ring and the Cp′ group on Ru1. The steric repulsion between the phenyl group and the Cp′ group on Ru2 is supported by the fact that the Ru1−Cp′(centroid) vector also tilts away from the μ_3-NPh group by 5° with respect to the Ru_3 plane. Such a "tilt" phenomenon was reported for several trinuclear

(14) Suzuki, H.; Kakigano, T.; Tada, K.; Igarashi, M.; Matsubara, K.; Inagaki, A.; Oshima, M.; Tanaka, M. Manuscript in preparation.

(15) Emsley, J., Ed. *The Elements*, 3rd ed.; Oxford University Press: New York, 1998; pp 142, 178.

(16) (a) Ru−N = 2.129 Å for $[(C_6H_5)(NH_3)_2ClRu](PF_6)$: Gould, R. O.; Jones, C. L.; Robertson, D. R.; Stephenson, T. A. *Cryst. Struct. Commun.* **1978**, *7*, 27. (b) Ru−N = 2.156 Å for $(NH_3)_5\{(CH_3)SO\}$: March, F. C.; Feruson, G. *Can. J. Chem.* **1971**, *49*, 3590.

(17) Ilan, Y.; Kapon, M. *Inorg. Chem.* **1986**, *25*, 2350.

(18) (a) 2.053 Å for $\{Ru(CO)_3\}_3(\mu_3\text{-}NPh)$: Bhaduri, H.; Gopalkrishnan, K. S.; Sheldrick, G. M.; Clegg, W.; Stalke, D. *J. Chem. Soc., Dalton Trans.* **1983**, 2339. (b) 2.043 Å for $\{Ru(CO)_3\}_3(\mu_3\text{-}NC_6H_4OCH_3)(\mu\text{-}H_2)$: Lausarot, P. M.; Operti, L.; Vaglio, G. A.; Valle, M.; Tiripicchio, A.; Camellini, M. T.; Graiboldi, P. *Inorg. Chim. Acta* **1986**, *103*, 122.

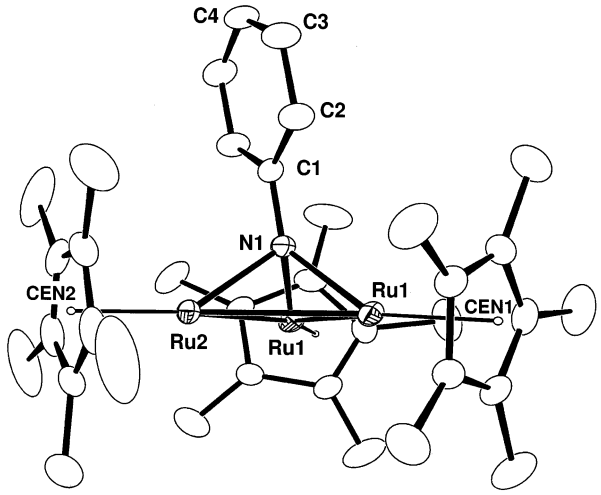

Figure 4. Molecular structure of **4**. Thermal ellipsoids are drawn at the 30% probability level.

Table 4. Selected Interatomic Distances (Å) and Angles (deg) of 4[a]

	Distances		
Ru1−Ru1	2.7226(16)	Ru2−N1	2.013(4)
Ru1−Ru2	2.729(9)	N1−C1	1.408(6)
Ru1−N1	2.0243(3)		
	Angles		
Ru2−N1−Ru1	85.10(12)	C1−N1−Ru1	132.92(14)
Ru1−N1−Ru1	84.53(14)	C1−N1−Ru2	119.7(3)
N1−Ru1−Ru2	42.27(10)	G1−Ru1−CEN1	174.0
N1−Ru2−Ru1	47.63(8)	G1−Ru2−CEN2	177.8

[a] G1 is the center of the gravity of the Ru_3 triangle, and CEN1 and CEN2 are the centroids of Cp′.

μ_3-phenylimido complexes, such as $Ru_3(CO)_9(\mu\text{-}H)_2(\mu_3\text{-}NPh)$[19] and $Ru_3(CO)_6(\eta^6\text{-}C_6H_6)(\mu_3\text{-}NPh)$.[20]

The structure shown in Figure 4 is consistent with the spectral data of the monocapped imido complex **4**. The molecule has a crystallographic symmetry plane with C4, C1, N1, and Ru2. Since complex **4** is a 48e cluster, as are **2** and **3**, the Ru−Ru bond is also required to be a single bond according to the EAN rule. The average Ru−Ru distance is 2.726 Å, which is almost the same as those of the bicapped imido complexes **2** and **3**. The Ru1−N1 and Ru2−N1 distances of 2.024(3) and 2.013(4) Å, respectively, are also comparable to those observed in **2** and **3**. As observed in the structure of **3**, the phenyl group bound to N1 tilts toward Ru2. The C1−N1−Ru1 and the C1−N1−Ru1 angles are 132.9(1) and 119.7(3)°, respectively. Release of steric repulsion between the hydrogen at the ortho position and the Cp′ group attached to Ru1 is most likely responsible for the tilt of the phenyl group. As anticipated from the repulsive interaction between the phenyl group and the Cp′ group on the Ru2, the Ru2−Cp′(centroid) vector also tilts away from the μ_3-NPh group by 2.2° with respect to the Ru_3 plane. The corresponding tilt angle of 6.0° for the Ru1−Cp′(centroid) vector is significantly larger than that of the Ru2−Cp′(centroid) vector.

There is no significant difference in the Ru−Ru bond lengths between the bicapped imido complex and the monocapped complex.

(19) Bhaduri, S.; Gopalkrishnan, K. S.; Clegg, W.; Stalke, D. *J. Chem. Soc., Dalton Trans.* **1984**, 1765.
(20) Basu, A.; Bhaduri, S.; Khwaja, H.; Meyer-Base, K.; Sheldrick, G. M. *J. Chem. Soc., Dalton Trans.* **1986**, 2501.

Table 5. Activation Parameters

substrate	E_a (kcal/mol)	$\Delta H^{\ddagger}$ (kcal/mol)	$\Delta S^{\ddagger}$ (cal/(mol K))
$PhNHNH_2$	19.6(1.7)	18.9(1.7)	−22.7(4.7)
$MeNHNH_2$	12.9(2.0)	12.2(2.0)	−40.8(5.6)
PhNHNHPh	10.5(0.3)	9.8(0.3)	−50.1(0.9)
Me_2NNH_2[a]	20.4(3.0)	19.6(3.0)	−23.0(8.7)
PhN=NPh[b]	9.04(0.6)	8.3(0.6)	−54.5(1.7)

[a] Reference experiment, which predominantly yields the bis(μ_3-NH) complex. [b] Reference experiment, which yields the μ_3-NPh complex predominantly together with a small amount of bis(μ_3-NPh) complex.

Mechanistic Aspects of the Reaction of 1 with Methylhydrazine, Phenylhydrazine, and 1,2-Diphenylhydrazine. A notable feature of the reactions of the triruthenium pentahydride **1** with substituted hydrazines is that their reaction paths are specific to the substitution mode of the hydrazine derivatives. In the reaction with monosubstituted hydrazine, mixed-bicapped μ_3-imido complexes are exclusively formed, while the reaction with 1,2-diphenylhydrazine results in the predominant formation of the monocapped μ_3-imido complex. To elucidate the mechanism of the reaction of **1** with mono- and disubstituted hydrazines, kinetic studies were performed.

The reaction of **1** with an excess amount (10−30 equiv) of hydrazine derivatives in tetrahydrofuran-d_8 was monitored by means of ^{1}H NMR spectroscopy at various temperatures. As mentioned above, reaction intermediates were detected in the reactions with both methylhydrazine and phenylhydrazine. This shows that the rate-determining step is the second step that involves conversion of the intermediate into the final product, **2** or **3**. On the other hand, the reaction of **1** with 1,2-diphenylhydrazine directly produces **4** without formation of any intermediary species. Since the kinetic studies were performed by monitoring the concentration of **1**, the estimated activation parameters for the reaction with methylhydrazine and phenylhydrazine are assigned to those for the step to the intermediates. Regardless of the hydrazine derivatives used in the reaction, the rate law is pseudo first order in the pentahydride cluster **1**. The estimated kinetic parameters for the reactions with phenylhydrazine, methylhydrazine, and 1,2-diphenylhydrazine are listed in Table 5 together with those for the reactions with 1,1-dimethylhydrazine and azobenzene as the references.

The reactions are roughly classified into two groups on the basis of the activation parameters. The activation enthalpy is relatively small (ca. 10 kcal/mol) and the activation entropy is a large negative value (−40 to −55 eu) for the reaction with methylhydrazine, 1,2-diphenylhydrazine, and azobenzene. In contrast, the values of activation entropy and activation enthalpy are ca. −23 eu and 18−20 kcal/mol, respectively, for the reaction with phenylhydrazine and 1,1-dimethylhydrazine.

The large negative values of activation entropy for the reactions with methylhydrazine, 1,2-diphenylhydrazine, and azobenzene imply that the capture of substrates in the reaction site is most likely the rate-determining step. The similarity in the activation parameters for methylhydrazine and 1,2-diphenylhydrazine convinces us that the methylhydrazine molecule is captured in the reaction site from the −NHMe terminus in preference to the $-NH_2$ terminus, despite its bulkiness. This is

probably the result of enhancement of nucleophilicity at the nitrogen atom due to introduction of an electron-releasing methyl group. On the other hand, the small absolute values of activation entropy for the reactions of phenylhydrazine and 1,1-dimethylhydrazine indicate that the hydrazine molecule is most probably captured into the Ru_3 core from the less bulky $-NH_2$ terminus rather than the bulky −NPhH and $-NMe_2$ termini.

To shed light on the reaction mechanism of the formation of the mixed-bicapped imido complexes **2** and **3**, the reaction of the mono-μ_3-NH complex $(Cp'Ru)_3(\mu_3\text{-}NH)(\mu\text{-}H)_3$ (**8**), which is one of the possible intermediates, with phenylhydrazine or methylhydrazine was examined. The μ_3-NH complex **8** was independently prepared by the reaction of **1** with Me_3SiN_3 in the presence of methanol.[13] The reaction of **8** with 10 molar equiv of methylhydrazine in tetrahydrofuran at 100 °C quantitatively yielded the bis-μ_3-NH complex $(Cp'Ru)_3(\mu_3\text{-}NH)_2(\mu\text{-}H)$ (**6**) (eq 4). The reaction of **8** with 20 equiv

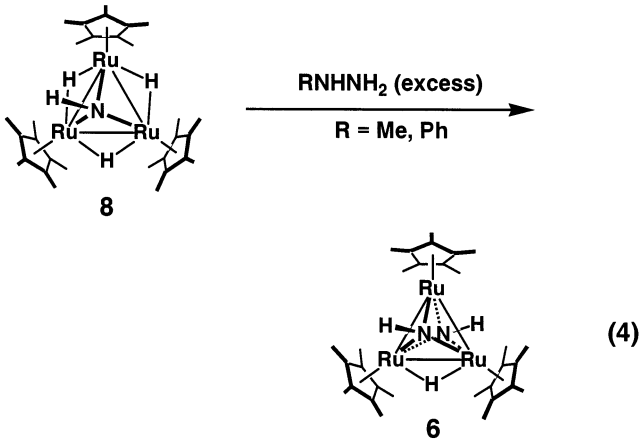

(4)

of phenylhydrazine in tetrahydrofuran also resulted in the exclusive formation of **6**. Complex **6** is a new compound and was identified by means of infrared spectroscopy and ^1H and ^{13}C NMR spectroscopy as well as the microanalytical data, as shown in the Experimental Section. A characteristic feature of the ^1H NMR spectral data is the chemical shift of the hydride ligands. The chemical shift of δ −19.27 for the hydride ligand is very similar to those observed in the bis(μ_3-imido) complexes **2**, **3**, and **5**.

The molecular structure of **6**, determined by an X-ray diffraction study, is illustrated in Figure 5, and relevant geometrical parameters are given in Table 6. Crystallographic data and results of the analyses are listed in Table 1.

The structure shown in Figure 5 clearly demonstrates the structural identity of **6**, which has two triply bridging imido groups on both faces of the Ru_3 core.

It is noteworthy that the symmetrically capped bis-(μ_3-imido) complex **6** is the sole product and no mixed-bicapped imido complex, **2** or **3**, is formed at all in the reaction of **8** with methylhydrazine or phenylhydrazine. This result clearly shows that the mixed-bicapped imido complexes **2** and **3** are not formed by the reaction of **8** with methylhydrazine or phenylhydrazine, although complex **8** is considered to be one of the possible intermediates.

The mono-μ_3-NPh-capped complex **4** seems to be one of the possible intermediates in the reaction of **1** with

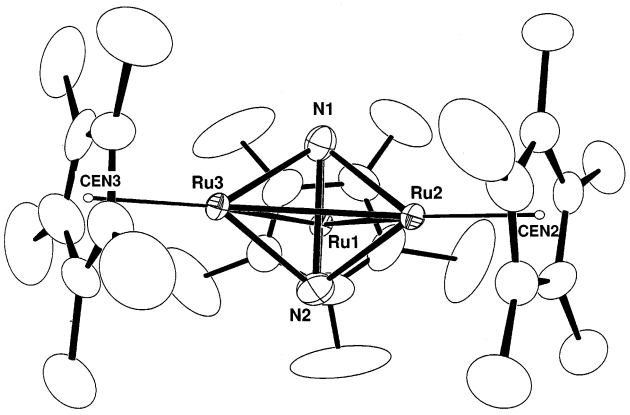

Figure 5. Molecular structure of **6**. Thermal ellipsoids are drawn at the 30% probability level.

Table 6. Selected Interatomic Distances (Å) and Angles (deg) of 6[a]

	Distances		
Ru1−Ru2	2.7391(10)	Ru2−N1	2.024(10)
Ru2−Ru3	2.7476(10)	Ru2−N2	1.967(11)
Ru3−Ru1	2.7393(11)	Ru3−N1	1.999(10)
Ru1−N1	2.017(10)	Ru3−N2	2.023(10)
Ru1−N2	1.999(11)		
	Angles		
Ru1−N1−Ru2	85.4(4)	Ru3−N2−Ru1	85.8(4)
Ru2−N1−Ru3	86.2(4)	G1−Ru1−CEN1	179.21
Ru3−N1−Ru1	86.0(4)	G1−Ru2−CEN2	179.12
Ru1−N2−Ru2	87.3(4)	G1−Ru3−CEN3	177.16
Ru2−N2−Ru3	87.0(4)		

[a] G1 is the center of the gravity of the Ru_3 triangle, and CEN is the centroid of Cp′.

phenylhydrazine. We carefully examined the possibility that the reaction proceeded by way of **4** through the reaction of **4** with phenylhydrazine. While the reaction of **1** with phenylhydrazine at 100 °C was complete within 6 h to yield **3** quantitatively, the reaction of **4** with phenylhydrazine was much slower than that of **3** and the yield of **3** was ca. 72%, despite the elongation of the reaction time (100 °C, 3 days) (eq 5). These results

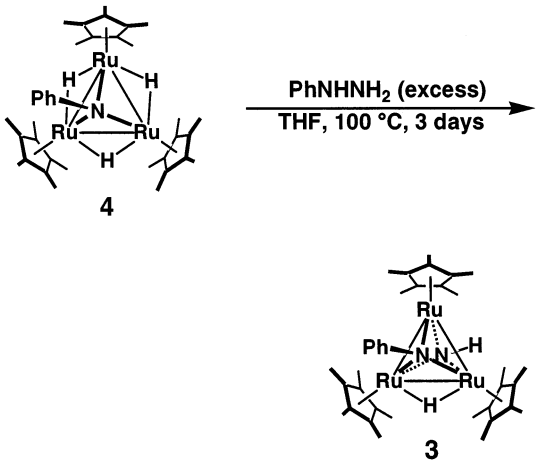

(5)

strongly indicate that the mono(phenylimido) complex **4** is not the intermediate of the formation of bis(imido complexes **3** and **5**.

Therefore, it is likely that both of the two μ_3-imido ligands introduced into the Ru_3 core of **2** and **3** are derived from one molecule of the monosubstituted

Scheme 1. Plausible Mechanism for the Reaction of 1 with Substituted Hydrazines

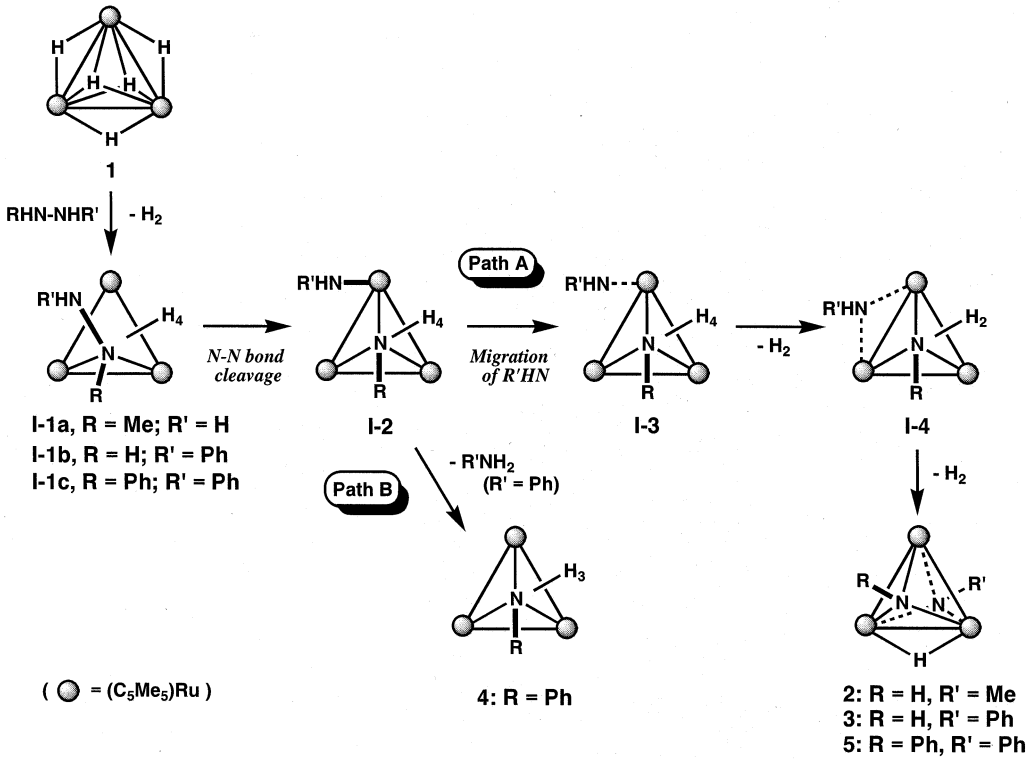

hydrazine. Namely, both of the two amino fragments, $-NH_2$ and $-NHR$, derived from the same hydrazine molecule are converted to the μ_3-imido ligands as they stay inside the coordination sphere.

On the basis of these observations, we propose one plausible reaction path that involves nitrogen−nitrogen bond cleavage and subsequent ligand migration to the opposite face of the Ru_3 plane (Scheme 1).

In the reaction of **1** with phenylhydrazine, the hydrazine molecule is most probably captured in the reaction site of **1** from the less bulky NH_2 terminus. In contrast, methylhydrazine is taken in the Ru_3 core from the bulky but more nucleophilic $-NHMe$ terminus. After the incorporation of the monosubstituted hydrazine molecule into the Ru_3 site, a nitrogen−hydrogen bond would be cleaved to yield a bridging hydrazido(1−) complex, $(Cp'Ru)_3(\mu\text{-}NMeNH_2)(\mu\text{-}H)_4$ (**I-1a**) or $(Cp'Ru)_3(\mu\text{-}NHNHPh)(\mu\text{-}H)_4$ (**I-1b**). Then the nitrogen−nitrogen bond of the μ-hydrazido(1−) ligand in **I-1a** and **I-1b** is cleaved to yield the amido−μ_3-imido intermediate **I-2**. Coordination of the β-nitrogen atom of the μ-hydrazido ligand in **I-1** to the third ruthenium atom would promote the cleavage of the nitrogen−nitrogen bond. Migration of the NHR′ fragment to the opposite face of the Ru_3 plane to lead to **I-3** (path A) and bridging coordination of the NHR′ group together with liberation of dihydrogen affords the intermediate **I-4**. There have been several precedents of migration of an organic group from one side to the opposite side with respect to the molecular plane of the trinuclear metal cluster.[21] When the reaction of **1** with phenylhydrazine was monitored by means of ^1H NMR spectroscopy, the intermediate **I-4** was detected. Subsequent N−H bond cleavage would generate the mixed-bicapped imido complex **2** or **3**. The NHR′ fragment likely remained inside of the coordination sphere of the trinuclear hydride complex throughout these steps.

In the case of 1,2-diphenylhydrazine, it cannot enter the reaction site of **1** as freely as the monosubstituted hydrazine because of the bulkiness of the substituent on the nitrogen atom. Therefore, the capture of 1,2-diphenylhydrazine should be a rate-determining step. The μ-hydrazido(2−) complex **I-1c** undergoes cleavage of the nitrogen−nitrogen bond to generate **I-2**. The reaction site of **I-2** is likely too congested, with the bulky substituent on the triply bridging nitrogen atom, to leave the phenylamido fragment (−NHPh) inside the reaction site. Reductive elimination of aniline from **I-2** would lead to the final product **4** (path B); otherwise, migration of the R′NH group to the opposite plane and subsequent dehydrogenation would lead to the formation of bis(imido) complex **5**.

Conclusion

A metal polyhydride cluster has many hydrogen atoms in the molecule and the intrinsic ability to transfer multiple electrons between the cluster and the coordinated substrate. Therefore, a polyhydride cluster likely promotes nitrogen reduction to ammonia in the absence of both a proton source and a reducing agent. We have proved that the triruthenium pentahydride complex $(Cp'Ru)_3(\mu\text{-}H)_3(\mu_3\text{-}H)_2$ (**1**) reacted with hydrazine derivatives in the absence of a proton source and a reducing agent to result in the production of a mono(μ_3-imido) or bis(μ_3-imido) complex selectively as a result of the nitrogen−nitrogen bond cleavage.

The reaction of **1** with a monosubstituted hydrazine such as methylhydrazine and phenylhydrazine resulted

(21) (a) Takemori, T.; Inagaki, A.; Suzuki, H. *J. Am. Chem. Soc.* **2001**, *123*, 1762. (b) Adams, K. J.; Barker, J. J.; Knox, S. A. R.; Orpen, A. G. *J. Chem. Soc., Dalton Trans.* **1996**, 975.

in the exclusive formation of the nonsymmetrically capped bis(μ_3-imido) complex (Cp′Ru)$_3$(μ_3-NR)(μ_3-NH)(μ-H) (**2**, R = Me; **3**, R = Ph). This shows that both of the two amino fragments, −NH$_2$ and −NHR, derived from the same hydrazine molecule, are converted to μ_3-imido ligands as they stay inside the coordination sphere of **1**. In the reaction of **1** with phenylhydrazine, the intermediary μ-phenylamido−μ_3-imido complex (Cp′Ru)$_3$(μ-NPhH)(μ_3-NH)(μ-H) (**I-4**) was detected by means of ^{1}H NMR spectroscopy. In contrast to the reaction with monosubstituted hydrazine, the reaction of **1** with 1,2-diphenylhydrazine predominantly yields the monocapped imido complex (Cp′Ru)$_3$(μ_3-NPh)(μ-H)$_3$ due to the steric hindrance between the Cp′ groups surrounding the reaction site of **1** and the incoming bulky 1,2-diphenylhydrazine.

To elucidate the mechanism of the reaction of **1** with mono- and disubstituted hydrazines, kinetic studies were performed. As a result, we have proposed a mechanism involving nitrogen−nitrogen bond cleavage caused by cooperative action due to the three ruthenium centers.

Experimental Section

General Considerations. The compounds described below were handled under an argon atmosphere with rigorous exclusion of air and water using Schlenk techniques. Dehydrated solvents were purchased from Kanto Chemical Co., Inc. (Cat. No. 41001-85 for tetrahydrofuran, 40500-85 for toluene, and 32053 for pentane). Methylhydrazine, phenylhydrazine, and diphenylhydrazine were obtained from Tokyo Kasei Kogyo Co., Ltd., and no further purification was performed. (Cp′Ru)$_3$(μ_3-H)$_2$(μ-H)$_3$ (**1**) was prepared as previously described.[14] Benzene-d_6 and tetrahydrofuran-d_8 were distilled, dried over sodium benzophenone ketyl, and stored under an argon atmosphere. ^{1}H and ^{13}C NMR spectra were recorded on a Varian INOVA 400 Fourier transform spectrometer with tetramethylsilane as an internal standard. Elemental analyses were performed on a Perkin-Elmer 2400 II instrument. IR spectra were recorded on a Nicolet Avatar 360 spectrometer. GC-mass spectra were obtained by means of a Shimadzu GC 17A instrument using a DB-5 column and GCMS-QP5000 as a detector.

Reaction of 1 with Methylhydrazine: Formation of (Cp′Ru)$_3$(μ_3-NMe)(μ_3-NH)(μ-H) (2). A THF solution (5 mL) of **1** (26.3 mg, 0.0368 mmol) was charged in a 50 mL Schlenk tube, to which was added methylhydrazine (20 μL, 0.357 mmol). The mixture was stirred at 100 °C for 96 h, and the solution turned red-yellow. After removal of the solvent under reduced pressure, the residue was extracted with toluene and purified by column chromatography on alumina using toluene as the eluent. The red solid of **2** (20.9 mg, 0.0277 mmol, 75%) was obtained by removal of the solvent under reduced pressure. Red crystals of **2** suitable for an X-ray diffraction study were grown by slow evaporation of a concentrated THF solution at −30 °C. **2**: ^{1}H NMR (400 MHz, room temperature, C_6D_6, δ/ppm) −19.15 (s, 1H, Ru−*H*), 1.79 (s, 30H, Cp′−*Me*), 1.85 (s, 15H, Cp′−*Me*), 4.24 (s, 3H, N−C*H*$_3$), 13.06 (br s, $w_{1/2}$ = 59.3 Hz, 1H, μ_3-N*H*); ^{13}C NMR (100 MHz, room temperature, C_6D_6, δ/ppm) 12.3 (q, J_{CH} = 125.7 Hz, Cp′ *Me*), 13.4 (q, J_{CH} = 124.6 Hz, Cp′ *Me*), 59.3 (dq, J_{CH} = 134.6 Hz, J = 3.9 Hz, N−*C*H$_3$), 82.4 (s, Cp ring), 92.9 (s, Cp′ ring); IR (ATR, cm^{-1}) 2964, 2897, 2822, 1474, 1452, 1429, 1375, 1368, 1103, 1069, 1020, 870, 798, 626. Anal. Calcd for $C_{31}H_{50}N_2Ru_3$: C, 49.38; H, 6.68; N, 3.72. Found: C, 49.10; H, 6.42; N, 3.72.

Reaction of 1 with Phenylhydrazine: Formation of (Cp′Ru)$_3$(μ_3-NPh)(μ_3-NH)(μ-H) (3). Phenylhydrazine (30 μL, 0.295 mmol) was added to a solution of **1** (9.8 mg, 0.0137 mmol) in 5 mL of tetrahydrofuran. The reaction mixture was stirred for 6 h at 100 °C. Removal of the solvent under reduced pressure gave a red solid of **3**. The solid was extracted with toluene and purified by column chromatography on alumina using toluene as the eluent. After removal of the solvent in vacuo, 7.7 mg (0.009 41 mmol) of **3** was obtained. Red crystals of **3** suitable for an X-ray diffraction study were grown by slow evaporation of a concentrated THF solution at −30 °C. **3**: ^{1}H NMR (400 MHz, room temperature, THF-d_8, δ/ppm) −18.93 (s, 1H, Ru−*H*), 1.64 (s, 15H, Cp′ *Me*), 1.74 (s, 30H, Cp′ *Me*), 6.73 (t, 1H, J = 7.2 Hz, *p*-*H*), 6.83 (d, 2H, J = 7.2 Hz, *o*-*H*), 6.97 (t, 2H, J = 8.0 Hz, *m*-*H*), 13.67 (br s, $w_{1/2}$ = 34.1 Hz, 1H, μ_3-N*H*); ^{13}C NMR (100 MHz, room temperature, THF-d_8, δ/ppm) 11.9 (q, J_{CH} = 125.4 Hz, Cp′ *Me*), 12.7 (q, J_{CH} = 124.9 Hz, Cp′ *Me*), 89.1 (s, Cp′ ring), 91.2 (s, Cp′ ring), 120.9 (d, J_{CH} = 155.4, para), 123.5 (d, J_{CH} = 158.5 Hz, ortho), 127.8 (d, J_{CH} = 153.9 Hz, meta), 170.7 (s, ipso); IR (ATR, cm^{-1}) 2963, 2902, 2279, 1583, 1474, 1371, 1259, 1089, 1018, 787, 643. Anal. Calcd for $C_{31}H_{50}N_2Ru_3$: C, 52.99; H, 6.42; N, 3.43. Found: C, 52.46; H, 6.75; N, 3.45.

Monitoring the Reaction of 1 with Phenylhydrazine: Determination of Intermediate. An NMR tube was charged with **1** (4.2 mg, 0.005 88 mmol), tetrahydrofuran-d_8 (0.4 mL), and cyclooctane (6.4 μL, 0.0470 mmol). After addition of phenylhydrazine (20 μL, 0.200 mmol), the sample tube was sealed and heated at 100 °C. The change of the intensity ratio of the signals of Cp′ to that of cyclooctane as an internal standard was monitored by means of ^{1}H NMR spectroscopy. After 50 min, the distribution of complex **1**, the intermediate **X**, and **3**, whose distributions were 28%, 41%, and 31%, respectively, were detected. The intermediate **X** was identified on the basis of the ^{1}H and ^{13}C NMR spectra. **X**: ^{1}H NMR (400 MHz, room temperature, THF-d_8, δ/ppm) −19.30 (s, 2H, Ru−*H*), 1.49 (s, 15H, Cp′ *Me*), 1.96 (s, 30H, Cp′ *Me*), 7.00 (*p*-*H*), 7.16 (t, 2H, J = 7.8 Hz, *m*-*H*), 7.70 (t, 2H, J = 8.0 Hz, *o*-*H*) (no signals are observed for N-*H*); ^{13}C NMR (100 MHz, room temperature, THF-d_8, δ/ppm) 10.8 (q, J_{CH} = 125.4 Hz, Cp′ *Me*), 13.7 (q, J_{CH} = 124.9 Hz, Cp′ *Me*), 88.5 (s, Cp′ ring), 92.2 (s, Cp′ ring), 121.9 (s, para), 127.5 (s, meta), 128.3 (s, ortho), 171.2 (s, ipso).

The signal observed at δ_H 7.00 was assigned as *p*-H on the basis of the HMQC spectra. HMQC (room temperature, THF-d_8): δ_C 128.3, δ_H 7.70; δ_C 127.5, δ_H 7.16; δ_C 121.9, δ_H 7.0. The COSY spectrum measured in tetrahydrofuran-d_8 at room temperature revealed the relationship between the two peaks at δ 7.70 and 7.16.

Reaction of 1 with 1,2-Diphenylhydrazine: Formation of (Cp′Ru)$_3$(μ_3-NPh)(μ-H)$_3$ (4) and (Cp′Ru)$_3$(μ_3-NPh)$_2$(μ-H) (5). An NMR tube was charged with **1** (7.3 mg, 0.0139 mmol), 1,2-diphenylhydrazine (18.8 mg, 0.102 mmol), and tetrahydrofuran-d_8 (0.4 mL) and sealed. The sample tube was heated at 100 °C. After the mixture was heated for 30 h, the solution turned green. The ^{1}H NMR spectrum revealed the formation of a 91:9 mixture of **4** and **5**. This ratio was based on the integral intensity of the Cp′ region in the ^{1}H NMR spectrum. Recrystallization from the mixed solvent of toluene and a small amount of pentane at −30 °C yielded analytically pure green crystals of **4**. **4**: ^{1}H NMR (400 MHz, room temperature, THF-d_8, δ/ppm) −13.37 (s, 3H, Ru−*H*), 1.72 (s, 45H, Cp′ *Me*), 6.59 (d, 2H, J = 7.6 Hz, *o*-H), 6.70 (t, 1H, J = 6.8 Hz, *p*-*H*), 6.91 (t, 2H, J = 7.4 Hz, *m*-*H*); ^{13}C NMR (100 MHz, room temperature, THF-d_8, δ/ppm) 14.1 (q, J_{CH} = 125.4 Hz, Cp′ *Me*), 93.4 (s, Cp′ ring), 122.7 (d, J_{CH} = 173.8 Hz, ortho), 124.3 (d, J_{CH} = 144.7 Hz, meta), 128.7 (d, J_{CH} = 151.5 Hz, para), 173.7 (s, ipso); IR (ATR, cm^{-1}) 2962, 2900, 1583, 1474, 1450, 1260, 1091, 1019, 799. Anal. Calcd for $C_{36}H_{53}NRu_3$: C, 53.85; H, 6.65; N, 1.74. Found: C, 53.95; H, 6.45; N, 1.86.

5: ^{1}H NMR (400 MHz, room temperature, THF-d_8, δ/ppm) −18.76 (s, 1H, Ru−*H*), 1.39 (s, 15H, Cp′ *Me*), 1.72 (s, 30H, Cp′ *Me*), 6.84 (m, 2H, *p*-H), 7.03−7.08 (m, 8H, *o*- and *m*-*H*); ^{13}C NMR (100 MHz, room temperature, THF-d_8, δ/ppm) 11.5 (q,

J_{CH} = 125.6 Hz, Cp′ *Me*), 13.1 (q, J_{CH} = 125.6 Hz, Cp′ *Me*), 90.5 (s, Cp′ ring), 92.3 (s, Cp′ ring), 121.9 (d, J_{CH} = 157.4 Hz, para), 124.3 (d, J_{CH} = 157.8 Hz, meta), 127.4 (d, J_{CH} = 157.1 Hz, ortho), 169.1 (s, ipso).

Reaction of (Cp′Ru)$_3$(μ_3-NH)(μ-H)$_3$ (8) with Methylhydrazine. A 50 mL Schlenk tube was charged with **8** (40.1 mg, 0.0562 mmol) and tetrahydrofuran (5 mL). After 10 equiv of methylhydrazine (30 mL, 0.535 mmol) was added to the reaction mixture and this mixture stirred at 100 °C for 3 h, the solution turned red-yellow. Removal of the solvent under reduced pressure afforded (Cp′Ru)$_3$(μ_3-NH)$_2$(μ-H) (**6**) quantitatively, on the basis of the integral intensity of the hydride region in the ^{1}H NMR spectrum. **6**: ^{1}H NMR (400 MHz, room temperature, C_6D_6, δ/ppm): −19.27 (s, 1H, Ru−*H*), 1.85 (s, 15H, Cp′ *Me*), 1.92 (s, 30H, Cp′ *Me*), 12.98 (s, 1H, μ-N*H*); ^{13}C NMR (100 MHz, room temperature, C_6D_6, δ/ppm) 12.8 (q, J_{CH} = 125.1 Hz, Cp′ *Me*), 13.3 (q, J_{CH} = 124.7 Hz, Cp′ *Me*), 88.6 (s, Cp′ ring), 90.6 (s, Cp′ ring); IR (ATR, cm^{-1}) 2961, 2898, 2822, 1473, 1455, 1422, 1370, 1103, 1069, 1018, 886. Anal. Calcd for $C_{30}H_{48}N_2Ru_3$: C, 48.69; H, 6.54; N, 3.79. Found: C, 48.89; H, 6.24; N, 3.69.

Reaction of (Cp′Ru)$_3$(μ_3-NH)(μ-H)$_3$ (8) with Phenylhydrazine. An NMR tube was charged with **8** (7.3 mg, 0.0100 mmol) and tetrahydrofuran-d_8 (0.4 mL). After a large excess of phenylhydrazine (20 μL, 0.200 mmol) was added to the solution, the reaction mixture was heated at 100 °C for 3 days. The ^{1}H NMR spectrum showed the exclusive formation of the bis(μ_3-imido) complex **6**.

Reaction of (Cp′Ru)$_3$(μ_3-NPh)(μ-H)$_3$ (4) with Phenylhydrazine. An NMR tube was charged with **4** (26.5 mg, 0.033 mmol), phenylhydrazine (20 μL, 0.200 mmol), and tetrahydrofuran-d_8 (0.4 mL) and sealed. The reaction was carried out at 100 °C for 3 days. The solution changed to red-yellow. Complex **3** was formed in a yield of 72% on the basis of the integral intensity of the Cp′ region in the ^{1}H NMR spectra.

X-ray Structural Analyses of 2−4 and 6. Crystals of **2**−**4** and **6** were mounted on glass fibers. The diffraction data of **2** and **4** were collected on a Rigaku AFC7R four-circle diffractometer equipped with graphite-monochromated Mo Kα radiation (λ = 0.710 69 Å). Reflections were collected in the range 5° < 2θ < 55°. The intensity data were processed using the TEXSAN crystal structure analysis program package[22] operated on an IRIS Indigo computer. At the early stages of the refinement, the atomic scattering factors were obtained from the standard sources. In the reduction of the data, Lorentz/polarization corrections and empirical absorption corrections (ψ scan) were applied to the data.

The data of **3** and **6** were collected at −50 °C on an R-AXIS RAPID diffractometer. Data were collected in the ranges 3° < 2θ < 55° and 5° < 2θ < 55°, respectively, on oscillation images with an oscillation range of 3°. The readout was performed with a pixel size of 100 μm × 100 μm.

The structures of **2** and **4** were solved using Patterson methods and expanded using Fourier techniques. The structures of **3** and **6** were solved by direct methods using the SHELXS-97 program,[23] followed by successive cycles of full-matrix least-squares refinement on F^2. No H atoms bound to the Ru atom were observed in the Fourier maps, and the non-hydrogen atoms were refined anisotropically. Hydrogen atoms of methyl groups for **2**−**4** and **6** and phenyl groups for **3** and **4** were included in the structure factor calculations in idealized positions. Least-squares refinement was carried out using SHELXL-97.[23]

In the structure of **2**, one H atom attached to the Ru atom was disordered among the three Ru−Ru bonds, each of which had a population of 33.3%. The methylimido group was also disordered, one located on one side of the Ru_3 plane with an occupancy of 52.9% and the other on the opposite face with an occupancy of 47.1%, and hydrogens of the N-bound methyl group were not included. The final cycle of full-matrix least-squares refinement was based on 1760 observed reflections ($I > 2.00\sigma(I)$) and 117 variable parameters and converged with unweighted and weighted agreement factors of R = 0.0287 and R_w = 0.0721.

In the structure of **3**, one Cp′ ligand was disordered with an occupancy of 50:50, and it was refined isotropically. No H atoms of the disordered Cp′ ligand were generated. Moreover, one hydrogen atom was disordered among the three Ru−Ru bonds, each of which had a population of 33.3%. The final cycle of full-matrix least-squares refinement was based on 3170 observed reflections ($I > 2.00\sigma(I)$) and 171 variable parameters and converged with unweighted and weighted agreement factors of R = 0.0520 and R_w = 0.1214.

The structure of **4** was refined based on 3538 observed reflections ($I > 2.00\sigma(I)$) and 207 variable parameters. Refinement of positional and thermal parameters led to convergence with R = 0.0378, R_w = 0.1085, and GOF = 1.021.

Table 7. Reaction Conditions and Rate Constants for the Reaction of 1 with Methylhydrazine

run	temp, °C	amt of complex **1**, mg (concn, M)	amt of methylhydrazine, μL (concn, M)	rate constant, s^{-1}
1	70	6.6 (0.00924)	20 (0.893)	1.23×10^{-5}
2	80	6.3 (0.00882)	20 (0.893)	2.69×10^{-5}
3	90	6.5 (0.0910)	20 (0.893)	4.47×10^{-4}
4	100	10.9 (0.0153)	20 (0.893)	5.60×10^{-4}

Table 8. Reaction Conditions and Rate Constants for the Reaction of 1 with Phenylhydrazine

run	temp, °C	amt of complex **1**, mg (concn, M)	amt of phenylhydrazine, μL (concn, M)	rate constant, s^{-1}
1	70	8.7 (0.0305)	20 (0.501)	8.36×10^{-5}
2	80	3.6 (0.0126)	20 (0.501)	1.45×10^{-4}
3	90	5.5 (0.0193)	20 (0.501)	3.49×10^{-4}
4	100	8.6 (0.0120)	20 (0.501)	8.18×10^{-4}

Table 9. Reaction Conditions and Rate Constants for the Reaction of 1 with 1,2-Diphenylhydrazine

run	temp, °C	amt of complex **1**, mg (concn, M)	amt of 1,2-diphenylhydrazine, mg (concn, M)	rate constant, s^{-1}
1	70	5.2 (0.00728)	40.4 (0.219)	3.88×10^{-5}
2	80	8.1 (0.0113)	15.6 (0.0847)	6.13×10^{-5}
3	90	8.8 (0.0123)	24.9 (0.135)	9.45×10^{-5}
4	100	9.9 (0.0139)	18.8 (0.102)	1.33×10^{-4}

Table 10. Reaction Conditions and Rate Constant for the Reaction of 1 with 1,1-Dimethylhydrazine

run	temp, °C	amt of complex **1**, mg (concn, M)	amt of 1,1-dimethylhydrazine, μL (concn, M)	rate constant, s^{-1}
1	70	12.3 (0.0431)	20 (0.651)	1.79×10^{-5}
2	80	11.9 (0.0417)	20 (0.651)	6.84×10^{-5}
3	90	8.5 (0.0298)	20 (0.651)	1.01×10^{-4}
4	100	16.4 (0.0574)	20 (0.651)	2.23×10^{-4}

Table 11. Reaction Conditions and Rate Constant for the Reaction of 1 with Azobenzene

run	temp, °C	amt of complex **1**, mg (concn, M)	amt of azobenzene, mg (concn, M)	rate constant, s^{-1}
1	70	5.1 (0.00714)	11.9 (0.0653)	4.28×10^{-5}
2	80	7.8 (0.0109)	33.9 (0.186)	6.74×10^{-5}
3	90	8.6 (0.0120)	28.0 (0.385)	9.59×10^{-5}
4	100	6.3 (0.00882)	18.5 (0.102)	1.24×10^{-4}

(22) TEXSAN, Crystal Structure Analysis Package; Molecular Structure Corp., The Woodlands, TX, 1985 and 1992.

(23) Sheldrick, G. M. SHELX97, a computer program for crystal structure determination; University of Göttingen: Göttingen, Germany, 1997.

In the structure of **6**, all atoms were refined anisotropically. The final cycle of full-matrix least-squares refinement was based on 4962 observed reflections ($I > 2.00\sigma(I)$) and 332 variable parameters and converged with unweighted and weighted agreement factors of $R = 0.0777$ and $R_w = 0.1656$.

Crystal data and results of the analyses are listed in Table 1.

Kinetic Experiments on the Reaction of 1 with Hydrazines. Samples were prepared by weighing the appropriate quantities of **1** into NMR tubes and adding tetrahydrofuran-d_8 (0.4 mL) and an excess of substrates. The reactions were performed at 70, 80, 90, and 100 °C and monitored by measurement of the integral intensity of the Cp′ region in the ^{1}H NMR spectrum. The rate constants were calculated on the basis of the time conversion of [**1**] (Tables 7−11). The temperature dependence of the rate constants gave the activation parameters E_a, $\Delta H^{\ddagger}$, and $\Delta S^{\ddagger}$ (Table 5).

Acknowledgment. This work was partly supported by a Grant-in-Aid for Scientific Research on Priority Areas (No. 14078101, "Reaction Control of Dynamic Complexes") from the Ministry of Education, Science, Sports, and Culture, Japan. We acknowledge Kanto Chemical Co., Inc., for generous gifts of pentamethylcyclopentadiene.

Supporting Information Available: Tables of atomic coordinates and parameters, bond lengths and angles, torsion angles, and structure refinement details and ORTEP drawings of **2**−**4** and **6** with full numbering schemes; crystallographic data are also available in CIF format. This material is available free of charge via the Internet at http://pubs.acs.org.

OM020755+